Modulation of plasma membrane calcium-ATPase activity by local calcium microdomains near CRAC channels in human T cells

Diana M. Bautista and Richard S. Lewis

Department of Molecular and Cellular Physiology, Stanford University School of Medicine, Stanford, CA 94305, USA

The spatial distribution of Ca^{2+} signalling molecules is critical for establishing specific interactions that control Ca^{2+} signal generation and transduction. In many cells, close physical coupling of Ca^{2+} channels and their targets enables precise and robust activation of effector molecules through local $[Ca^{2+}]_i$ elevation in microdomains. In T cells, the plasma membrane Ca^{2+}-ATPase (PMCA) is a major target of Ca^{2+} influx through Ca^{2+} release-activated Ca^{2+} (CRAC) channels. Elevation of $[Ca^{2+}]_i$ slowly modulates pump activity to ensure the stability and enhance the dynamic nature of Ca^{2+} signals. In this study we probed the functional organization of PMCA and CRAC channels in T cells by manipulating Ca^{2+} microdomains near CRAC channels and measuring the resultant modulation of PMCAs. The amplitude and spatial extent of microdomains was increased by elevating the rate of Ca^{2+} entry, either by raising extracellular $[Ca^{2+}]$, by increasing the activity of CRAC channels with 2-aminoethoxyborane (2-APB), or by hyperpolarizing the plasma membrane. Surprisingly, doubling the rate of Ca^{2+} influx does not further increase global $[Ca^{2+}]_i$ in a substantial fraction of cells, due to a compensatory increase in PMCA activity. The enhancement of PMCA activity without changes in global $[Ca^{2+}]_i$ suggests that local $[Ca^{2+}]_i$ microdomains near CRAC channels effectively promote PMCA modulation. These results reveal an intimate functional association between CRAC channels and Ca^{2+} pumps in the plasma membrane which may play an important role in governing the time course and magnitude of Ca^{2+} signals in T cells.

(Received 17 December 2003; accepted after revision 12 February 2004; first published online 13 February 2004)
Corresponding author R. S. Lewis: Beckman Center B-111A, Stanford University School of Medicine, Stanford, CA 94305, USA. Email: rslewis@stanford.edu

Intracellular Ca^{2+} controls a remarkable breadth of processes within cells, including secretion, adhesion, motility, growth and differentiation. One of the challenges inherent to the use of such a promiscuous messenger is to maintain signalling specificity and thus optimize the information capacity of Ca^{2+} signals. The amplitude and spatial and temporal dynamics of Ca^{2+} signals are known to play important roles in achieving specificity in many cells. In neurones, the frequency of Ca^{2+} transients regulates differentiation, axon growth, and growth cone turning (Spitzer *et al.* 2000; Gomez *et al.* 2001). In lymphocytes, the amplitude, duration and frequency of Ca^{2+} signals has been shown to selectively activate specific transcriptional pathways (Dolmetsch *et al.* 1997, 1998).

Ca^{2+} signalling within local microdomains provides a further mechanism for generating specificity (Bootman *et al.* 2001). The diffusion of Ca^{2+} into the cytoplasm through channels in the plasma membrane and organelles creates local gradients of intracellular Ca^{2+} ($[Ca^{2+}]_i$). In these microdomains with volumes on the order of femtolitres, $[Ca^{2+}]_i$ can accumulate to levels that are orders of magnitude greater than the global average $[Ca^{2+}]_i$ measured throughout the cell. In this way voltage-gated Ca^{2+} channels in excitable cells act locally to trigger exocytosis (Augustine & Neher, 1992; Becherer *et al.* 2003), activate K^+ channels (Roberts, 1993; Prakriya *et al.* 1996), elicit Ca^{2+} release through ryanodine receptors (Cannell *et al.* 1995; Wang *et al.* 2001), and activate gene transcription pathways (Deisseroth *et al.* 1996; Dolmetsch *et al.* 2001). In a similar fashion, store-operated Ca^{2+} channels that open in response to Ca^{2+} store depletion are known to elicit local effects on Ca^{2+}-sensitive adenylate cyclases (Fagan *et al.* 1996, 1998), nitric oxide synthase (Lin

 DOI: 10.1113/jphysiol.2003.060004

et al. 2000) and mitochondria (Hoth *et al.* 1997) in non-excitable cells. In all of these examples, close positioning of Ca^{2+} channels and their targets may optimize the robustness, speed and selectivity of activating those targets.

The plasma membrane Ca^{2+}-ATPase (PMCA) is a target for Ca^{2+} influx in many cells, including T cells. Previous work has shown that the PMCA is the primary Ca^{2+} extrusion mechanism in T cells, where it functions to expel Ca^{2+} that has entered the cell through Ca^{2+} release-activated Ca^{2+} (CRAC) channels (Bautista *et al.* 2002). $[Ca^{2+}]_i$ elevation in T cells generates a biphasic increase in PMCA activity, consisting of a rapid increase due to binding to transport sites, followed by a slow enhancement, or modulation, resulting from a reduction in K_m and an increase in the V_{max} of the pump (Bautista *et al.* 2002). *In vitro* studies have shown that modulation of PMCA4b, the predominant isoform expressed in T cells (Caride *et al.* 2001), can occur through Ca^{2+}–calmodulin binding to a carboxy-terminal domain of the pump which displaces it from an autoinhibitory site near the catalytic domain (Carafoli, 1994; Caride *et al.* 1999). Modulation can increase PMCA activity severalfold in intact T cells, even at global $[Ca^{2+}]_i$ values that saturate the transport sites with Ca^{2+} (Bautista *et al.* 2002). In this way, modulation effectively increases the dynamic range of pump activity and helps guarantee the stability of Ca^{2+} control in the cell. Because modulation occurs slowly over tens of seconds, it also enhances Ca^{2+} dynamics, acting as a high-pass filter with memory.

In this study we examined the functional organization of PMCA and CRAC channels in Jurkat T cells. To test whether PMCAs respond to local gradients of $[Ca^{2+}]_i$ near open CRAC channels, we measured the dependence of PMCA modulation on the Ca^{2+} influx rate. Increasing the rate of Ca^{2+} entry by several methods enhanced PMCA modulation independently of changes in global $[Ca^{2+}]_i$, indicating that CRAC channels and PMCAs communicate through local microdomains. This close coupling has several important implications for the efficiency and magnitude of PMCA modulation as well as for the potential mechanisms underlying the organization of Ca^{2+} sources and sinks in the plasma membrane.

Methods

Cells and solutions

Experiments were performed with Jurkat E6-1, a human leukaemic T cell line (ATCC 1378; American Type Culture Collection, Rockville, MA, USA). Cells were grown in medium consisting of RPMI 1640 (Mediatech, Herndon, VA, USA) supplemented with 10% fetal calf serum (Hyclone, Logan, UT, USA), 1 mM L-glutamine, and 50 U ml^{-1} penicillin and 50 μg ml^{-1} streptomycin (Mediatech, Herndon, VA, USA). Cells were maintained in log-phase growth at 37°C and 6% CO_2. Extracellular Ringer solution contained (mM): 155 NaCl, 4.5 KCl, 2 or 20 $CaCl_2$, 1 $MgCl_2$, 10 D-glucose and 5 Na-Hepes (pH 7.4). For Ca^{2+}-free solution, 2 mM $MgCl_2$ and 1 mM EGTA were substituted for $CaCl_2$. The pipette solution for perforated-patch recording contained (mM): 115 caesium aspartate, 1 $CaCl_2$, 5 $MgCl_2$, 10 NaCl, and 10 Hepes (pH 7.2 with CsOH), plus 300 μg ml^{-1} amphotericin B (Sigma Chemical Co., St Louis, MO, USA). Thapsigargin (LC Biochemicals, Woburn, MA, USA) was diluted from a 1 mM stock in DMSO. 2-APB (Sigma) was diluted from a 5 mM stock in DMSO.

Video microscopic measurements of $[Ca^{2+}]_i$

Cells were loaded with 2 μM fura-2 AM Molecular Probes, Eugene, OR, USA) at 22–25°C for 25 min in culture medium and washed twice with fresh medium. Within 3 h of washing, cells were attached to poly-L-lysine-treated coverslip chambers on the stage of a Zeiss Axiovert 35 microscope equipped with a ×40 oil-immersion objective (Zeiss Achrostigmat, NA 1.3). Several minutes prior to imaging, cells were washed with Ringer solution. Cells were illuminated alternately at 350 nm and 380 nm for 132 ms every 2–5 s (bandpass filters from Chroma Technology, Brattleboro, VT, USA) using a Xe light source and filter wheel (Lambda LS and Lambda-10, Sutter Instruments, Novato, CA, USA). Fluorescence emission at $\lambda > 480$ nm (longpass filter from Chroma Technology) was captured with an intensified CCD camera (Hamamatsu Corp., Bridgewater, NJ, USA) and was digitized, background-corrected, and analysed with a VideoProbe imaging system (ETM Systems, Irvine, CA, USA) as described previously (Dolmetsch & Lewis, 1994). $[Ca^{2+}]_i$ was determined from background-corrected F_{350}/F_{380} ratio images (where F_{350} or F_{380} is the fluorescence intensity with 350 or 380 nm excitation, respectively) using the relation $[Ca^{2+}]_i = K^*(R - R_{min})/(R_{max} - R)$ (Almers & Neher, 1985), with values of K^*, R_{min} (fluorescence ratio in the absence of Ca^{2+}) and R_{max} (fluorescence ratio in the presence of saturating Ca^{2+}) measured in Jurkat cells *in situ* as previously described (Lewis & Cahalan, 1989). Analysis was conducted with automated routines written in Igor Pro (Wavemetrics, Lake Oswego, OR, USA). All pooled results are expressed as mean ± S.E.M. All experiments were conducted at 22–25°C.

Perforated-patch recording with simultaneous $[Ca^{2+}]_i$ measurements

Cells were loaded with 2 μM indo-1 AM in culture medium at 22–25°C for 30 min, washed, and attached to coverslip chambers on the stage of a Nikon Diaphot TMD microscope. Cells were excited at 360 nm (360/25 filter; Chroma Technology) for 50 ms every second through a Nikon ×40 Fluor objective (NA 1.3). The fluorescence at 405 nm and 485 nm (405/25 and 485/25 filters; Chroma Technology) was collected simultaneously with two photomultipliers (HC124-02, Hamamatsu). $[Ca^{2+}]_i$ was estimated from the relation $[Ca^{2+}]_i = K^*(R - R_{min})/(R_{max} - R)$, where R is the background-corrected 405/485 ratio. K^*, R_{min} and R_{max} were measured *in situ* as previously described (Zweifach & Lewis, 1995).

Recording pipettes were pulled from 100-μl capillaries (VWR Scientific Corp., South Plainfield, NJ, USA), coated with Sylgard (Dow Corning Corp., Midland, MI, USA), and fire-polished to resistances of 2–4 MΩ. Membrane current was recorded using an Axopatch 200 amplifier (Axon Instruments, Foster City, CA, USA), filtered at 2 kHz and digitized at a rate of 5 kHz. Command potentials and data collection were controlled by a Power Macintosh G3 computer (Apple, Cupertino, CA, USA) driving an ITC-16 interface (Instrutech Corp., Great Neck, NY, USA) using custom software extensions to Igor Pro. All command potentials were corrected for a measured liquid junction potential of −12 mV existing between the perforated-patch pipette solution and 2 mM Ca^{2+} Ringer solution. Access resistance in perforated-patch experiments varied from 4 to 6 MΩ.

Ca^{2+} release-activated Ca^{2+} current (I_{CRAC}) was measured at different holding potentials in the following way. The whole-cell current was averaged for 100-ms at the stated holding potential every 1 s, and 100 ms voltage ramps from −80 mV to +40 mV were applied every 10 s to confirm the stability of I_{CRAC} and the leak current (I_{leak}). I_{leak} was measured in response to voltage ramps in Ca^{2+}-free Ringer solution at the beginning and end of each experiment. I_{CRAC} was then determined at a given holding potential by subtracting the value of I_{leak} at that potential (obtained from the ramp currents) from the total average current.

Results

The main goal of this study was to assess whether PMCAs are modulated by local increases in $[Ca^{2+}]_i$ occurring near open CRAC channels. Although Ca^{2+} microdomains are far below the resolution limit of microscopic fura-2 measurements (see Discussion), we were able to address this question by asking whether conditions that alter the amplitude and spatial extent of these local gradients have effects on PMCA activity that are independent of changes in global cell $[Ca^{2+}]_i$.

Our experimental approach is illustrated in Fig. 1. Cells are first treated with 1 μM thapsigargin (TG) in Ca^{2+}-free Ringer solution to deplete Ca^{2+} stores fully and activate CRAC channels. Following full activation of CRAC channels, Ca^{2+} is added to the bath, leading to a rise in $[Ca^{2+}]_i$. As we have shown before, the $[Ca^{2+}]_i$ rise under these conditions is biphasic; slow up-regulation ('modulation') of PMCA activity by incoming Ca^{2+} allows $[Ca^{2+}]_i$ to reach a peak and then decline to a plateau level as the PMCA flux rate rises to match the rate of Ca^{2+} influx through CRAC channels (Bautista *et al.* 2002). After a steady-state level of modulation is achieved (within 300 s), extracellular Ca^{2+} ($Ca^{2+}{}_o$) is removed, and measurement of the clearance rate ($-d[Ca^{2+}]_i/dt$) gives an estimate of pump activity, which is solely responsible for clearance under these conditions (Bautista *et al.* 2002). After a rest period of 8−10 min in Ca^{2+}-free solution, PMCA modulation returns to resting levels (reversal time constant is ∼4 min; Bautista *et al.* 2002). A higher concentration of extracellular Ca^{2+} is then applied for another 300 s, and the resulting degree of PMCA activity is measured in a similar way following removal of $Ca^{2+}{}_o$. Under appropriate conditions (see below), a comparison of the clearance rates following the application of low and high $[Ca^{2+}]_o$ allows one to assess the relative degree of PMCA modulation under the two conditions.

The rate of Ca^{2+} clearance depends on $[Ca^{2+}]_i$ in several ways. PMCA activity is determined both by the occupancy of transport sites, which is a quasi-instantaneous function of $[Ca^{2+}]_i$, as well as by modulation, which is a time- and history-dependent function of $[Ca^{2+}]_i$. In addition, the rate of clearance is slowed by the buffering capacity of the cell, which acquires $[Ca^{2+}]_i$ dependence mostly from the buffering properties of the exogenous Ca^{2+} indicator, fura-2 (Bautista *et al.* 2002). To isolate the effect of $[Ca^{2+}]_i$ on modulation, we therefore compared clearance rates at approximately the same level of $[Ca^{2+}]_i$ following periods of exposure to low and high $[Ca^{2+}]_o$.

In the experiment of Fig. 1, we compared modulation by 0.5, 2 and 20 mM $Ca^{2+}{}_o$. Based on measurements of the Ca^{2+} dependence of I_{CRAC} in Jurkat cells (Premack *et al.* 1994), raising $[Ca^{2+}]_o$ from 0.5 mM to 2 mM should increase the influx rate by 2.5-fold, while raising $[Ca^{2+}]_o$ from 2 to 20 mM should further increase influx by 1.8-fold. On average, increasing $[Ca^{2+}]_o$ from 0.5 mM to 2 mM enhanced the clearance rate by 1.78-fold (±0.07, $n = 261$

cells; Fig. 1*A*). Further elevation of $[Ca^{2+}]_o$ from 2 to 20 mM augmented the clearance rate by 2.5-fold (± 0.1, $n = 261$ cells; Fig. 1*B*). Similar data were obtained in the presence of antimycin A1 (2 μM) and oligomycin (2 μM) to inhibit mitochondrial Ca^{2+} uptake, or when NaCl was replaced with NMDG, indicating that mitochondria and the Na^+–Ca^{2+} exchanger do not contribute significantly to the increased clearance following exposure to high $[Ca^{2+}]_o$. In addition, the increased clearance rate with high $[Ca^{2+}]_o$ is not due to an accumulation of modulation carried over from the first Ca^{2+} application, as similar results were obtained with a reversed order of solution changes, and the same solution presented twice produced identical amounts of modulation.

These results show that elevation of $[Ca^{2+}]_o$ enhances the modulation of the PMCA. When $[Ca^{2+}]_o$ is raised from 2 to 20 mM, the enhancement of modulation (2.5-fold) is dramatic given the rather small rise in global $[Ca^{2+}]_i$ (~20%). This non-linearity could result from an effect of local $[Ca^{2+}]_i$ elevation, or it could reflect a highly cooperative dependence of modulation on global $[Ca^{2+}]_i$. It is difficult from these data to distinguish the effects of local and global intracellular Ca^{2+}, because on average, increasing $[Ca^{2+}]_o$ elevates both.

One way to evaluate the effect of local $[Ca^{2+}]_i$ on modulation without interference from global $[Ca^{2+}]_i$ is shown in Fig. 1*C*. For the experiments shown in Fig. 1*A* and *B*, Ca^{2+} clearance rates were measured immediately following washout of $Ca^{2+}{}_o$, and the clearance rates for individual cells were plotted against their immediately preceding plateau $[Ca^{2+}]_i$ values. As discussed above, the clearance rate rises with $[Ca^{2+}]_i$ due not only to PMCA modulation but also to increased occupancy of PMCA transport sites and saturation of intracellular fura-2. However, it should be noted that local $[Ca^{2+}]_i$ gradients are unlikely to exist during measurements of the clearance

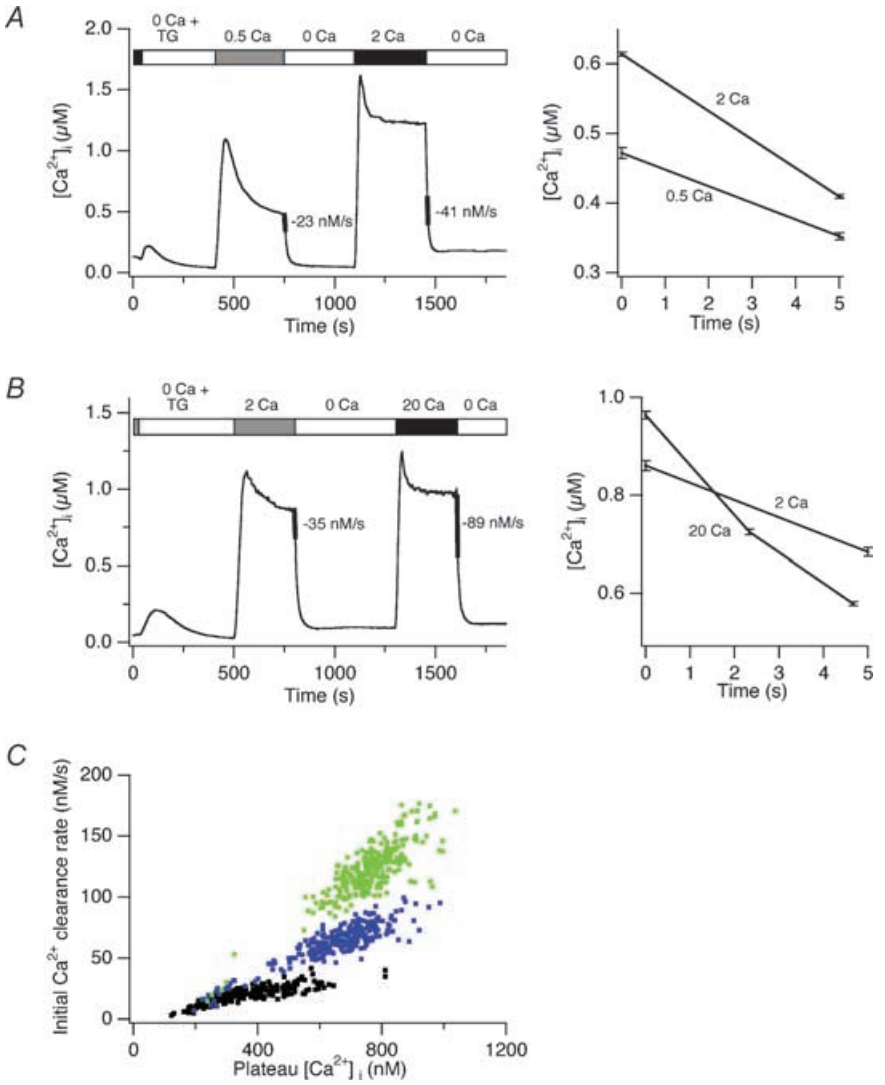

Figure 1. Effects of extracellular $[Ca^{2+}]$ on modulation of PMCA
TG (1 μM) was present in all solutions, beginning with 0 Ca^{2+} Ringer solution, as indicated, to deplete Ca^{2+} stores and activate CRAC channels. *A*, measurement of Ca^{2+} clearance rates following $[Ca^{2+}]_i$ elevation induced by 0.5 or 2 mM $Ca^{2+}{}_o$. The clearance rate at a common $[Ca^{2+}]_i$ following removal of $Ca^{2+}{}_o$ was measured by the $d[Ca^{2+}]_i/dt$ slopes over 5 s periods indicated by the thickened lines. The Ca^{2+} clearance data during these periods are overlaid on an expanded time scale to the right. Average response of 261 cells. Bars indicate S.E.M. in this and all subsequent figures. *B*, measurement of Ca^{2+} clearance rates following $[Ca^{2+}]_i$ elevation induced by 2 or 20 mM $Ca^{2+}{}_o$. Slopes were measured by linear regression over a 5 s period immediately following removal of $[Ca^{2+}]_o$ as indicated by the thickened lines. Data are overlaid and displayed on an expanded scale to the right. Average response of 261 cells. *C*, clearance rate in single cells as a function of $[Ca^{2+}]_i$ following long exposures to different $[Ca^{2+}]_o$. Data from the experiments in *A* and *B*. Each symbol represents the initial rate of Ca^{2+} clearance after removal of $Ca^{2+}{}_o$ plotted against the immediately preceding plateau $[Ca^{2+}]_i$ produced by 0.5 mM (black), 2 mM (blue) or 20 mM (green) $Ca^{2+}{}_o$. Each cell is represented by a pair of points (0.5 and 2 mM, or 2 and 20 mM).

rate (0 Ca^{2+}_o), because in the absence of influx diffusion will effectively equilibrate Ca^{2+} throughout the cell in the time scale of Ca^{2+} clearance (seconds). Thus, under these conditions both PMCA occupancy and Ca^{2+} buffering should be approximately equal among cells having the same global $[Ca^{2+}]_i$. Therefore, it is possible to estimate the degree of modulation separately from the effects of transporter occupancy and fura-2 saturation by comparing clearance rates in cells with a given level of $[Ca^{2+}]_i$. At 600 nM $[Ca^{2+}]_i$, for example, clearance rates increase as $[Ca^{2+}]_o$ is raised from 0.5 to 2 to 20 mM. As seen in Fig. 1*C*, this basic result applies at all steady-state $[Ca^{2+}]_i > 400$ nM. These results suggest that modulation is influenced by the driving force for Ca^{2+} entry, consistent with the idea that local $[Ca^{2+}]_i$ gradients contribute to this process.

However, comparing Ca^{2+} clearance among different cells in a population in this way may introduce complicating factors. For example, cells that reach a high level of $[Ca^{2+}]_i$ with low $[Ca^{2+}]_o$ may do so because of low pump expression or inefficient modulation of PMCA relative to cells that reach the same $[Ca^{2+}]_i$ with high $[Ca^{2+}]_o$. To avoid these potential complications, we developed several additional strategies (described below) to examine the role of local $[Ca^{2+}]_i$ gradients in PMCA modulation in individual cells.

Increasing $[Ca^{2+}]_o$ enhances PMCA modulation independently of global $[Ca^{2+}]_i$ in single cells

Surprisingly, in about 20% of TG-treated Jurkat cells, exposure to 2 and 20 mM $[Ca^{2+}]_o$ generates the same steady-state global $[Ca^{2+}]_i$ to within ± 10% ('iso-$[Ca^{2+}]_i$ response'; Fig. 2*A*). Thus, in these cells a comparison of the clearance rate in response to different levels of $[Ca^{2+}]_o$ can be used to test directly whether local Ca^{2+} gradients make a contribution to PMCA modulation. Figure 2*B* shows the average response to 2 and 20 mM Ca^{2+}_o, compiled from 64 cells that showed an iso-$[Ca^{2+}]_i$ response. Despite the fact that steady-state global $[Ca^{2+}]_i$ in these cells was equal under the two conditions, 20 mM Ca^{2+}_o elevated the clearance rate in every cell, by an average of 2.1 ± 0.26-fold compared to 2 mM Ca^{2+}_o. We observed comparable behaviour in freshly isolated human T cells (data not shown). Additional experiments in Jurkat cells using a low affinity Ca^{2+} indicator (fura-4F AM, $K_d = 770$ nM) also gave similar results, indicating that the equal plateau levels are not an artifact of fura-2 saturation at high $[Ca^{2+}]_i$. The enhanced PMCA activity under conditions of increased driving force and constant global $[Ca^{2+}]_i$ directly support an effect of local Ca^{2+} microdomains on the modulation process.

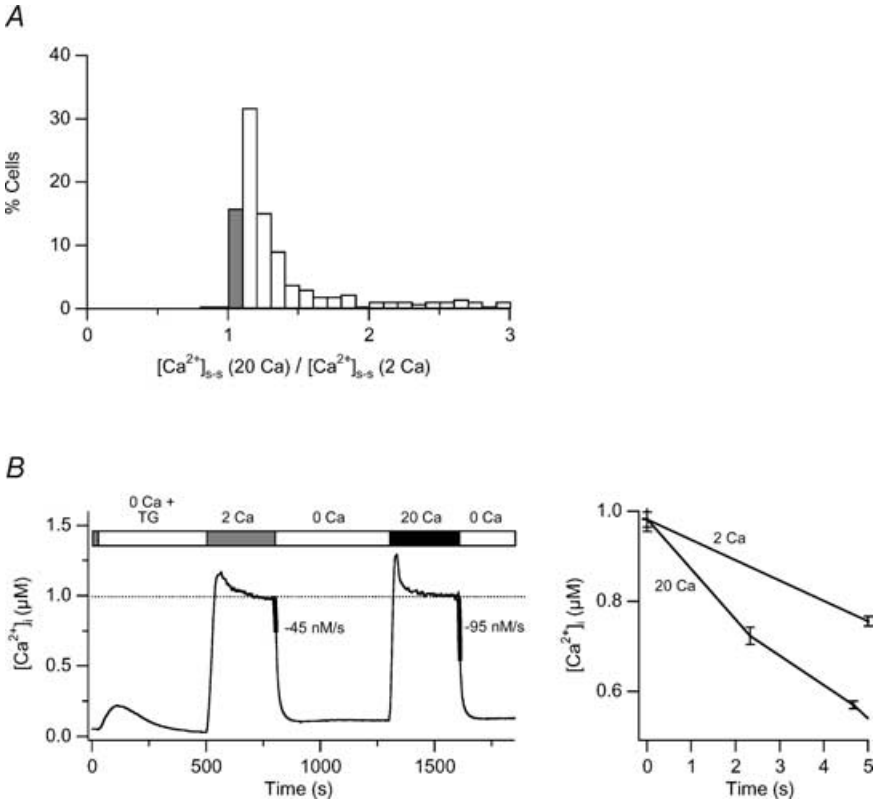

Figure 2. High $[Ca^{2+}]_o$ augments PMCA modulation independently of changes in global $[Ca^{2+}]_i$
TG-pretreated cells were exposed sequentially to 2 and 20 mM Ca^{2+}_o as shown in Fig. 1*B*. *A*, distribution of the plateau $[Ca^{2+}]_i$ levels generated by 20 mM Ca^{2+}_o relative to 2 mM Ca^{2+}_o in 265 individual cells. In 16% of the cells, 2 and 20 mM Ca^{2+}_o evoked the same global $[Ca^{2+}]_i$ plateau ('iso-$[Ca^{2+}]_i$' cells; shaded bar). *B*, average $[Ca^{2+}]_i$ responses from the iso-$[Ca^{2+}]_i$ cells identified in *A*. Ca^{2+} clearance rates indicated by the thickened lines were measured over the first 5 s following Ca^{2+}_o removal (left). Clearance was faster following exposure to higher $[Ca^{2+}]_o$, despite constant global $[Ca^{2+}]_i$. An overlay of the first 5 s of Ca^{2+} clearance following the 2 and 20 mM Ca^{2+}_o applications, highlights the different PMCA rates (right).

PMCA modulation by local $[Ca^{2+}]_i$ gradients is a widespread phenomenon

One question that arises from the iso-$[Ca^{2+}]_i$ cells is whether the local control of PMCA modulation is widespread, or whether it reflects the behaviour of only a minority of cells in the population. To gain a better idea of how common local control of PMCA modulation is, we used a CRAC channel blocker to equalize global $[Ca^{2+}]_i$ under conditions of increased driving force for Ca^{2+}. La^{3+} is a high-affinity blocker of the CRAC channel ($IC_{50} = 20$ nM; Aussel *et al.* 1996), inhibiting PMCA function only at much higher levels (50–100 μM; Carafoli, 1991). Thus, nanomolar concentrations of La^{3+} can be used to partially inhibit Ca^{2+} influx through CRAC channels without altering PMCA activity. The small size of the unitary CRAC current precludes direct confirmation of the kinetics of CRAC pore blockade by La^{3+}; however, we assume that blockade is probably similar to that seen in single-channel recordings of L-type voltage-gated Ca^{2+} channels (Lansman *et al.* 1986) based on the striking similarities in the ion selectivity properties and mechanisms of L-type channels and CRAC channels (Bakowski & Parekh, 2002; Prakriya & Lewis, 2002). Thus, by periodically blocking flux through the pore, La^{3+} is expected to reduce the globally averaged Ca^{2+} influx without altering the driving force for Ca^{2+} entry and hence the amplitude or extent of local $[Ca^{2+}]_i$ gradients. La^{3+} (7 nM) was added to the 20 mM Ca^{2+} solution to make the global $[Ca^{2+}]_i$ comparable to that observed with 2 mM Ca^{2+} alone (Fig. 3). About 70% of the cells displayed the same $[Ca^{2+}]_i$ plateau levels to within ± 10% under the two conditions (Fig. 3*A*). In all of these cells, PMCA-mediated extrusion was enhanced by 20 mM Ca^{2+} + La^{3+}, and on average modulation increased by 1.6-fold (± 0.11; $n = 373$; Fig. 3*B*). The somewhat lower degree of modulation seen here in comparison to Fig. 2 (1.6-*versus* 2.1-fold) may result from the shortened durations of microdomain 'events' caused by periodic channel blockade by La^{3+}. Most importantly, these results demonstrate that the effect of local $[Ca^{2+}]_i$ gradients on PMCA modulation is not restricted to a specialized subset of cells, but is a general feature of Jurkat cells.

2-APB enhances PMCA modulation through an effect of local Ca^{2+}

The evidence presented above for an effect of local $[Ca^{2+}]_i$ microdomains on PMCA modulation is based on experiments in which Ca^{2+} entry was enhanced by increasing $[Ca^{2+}]_o$. However, in some cells $Ca^{2+}{}_o$ in the range of 0.5–10 mM is known to bind to and

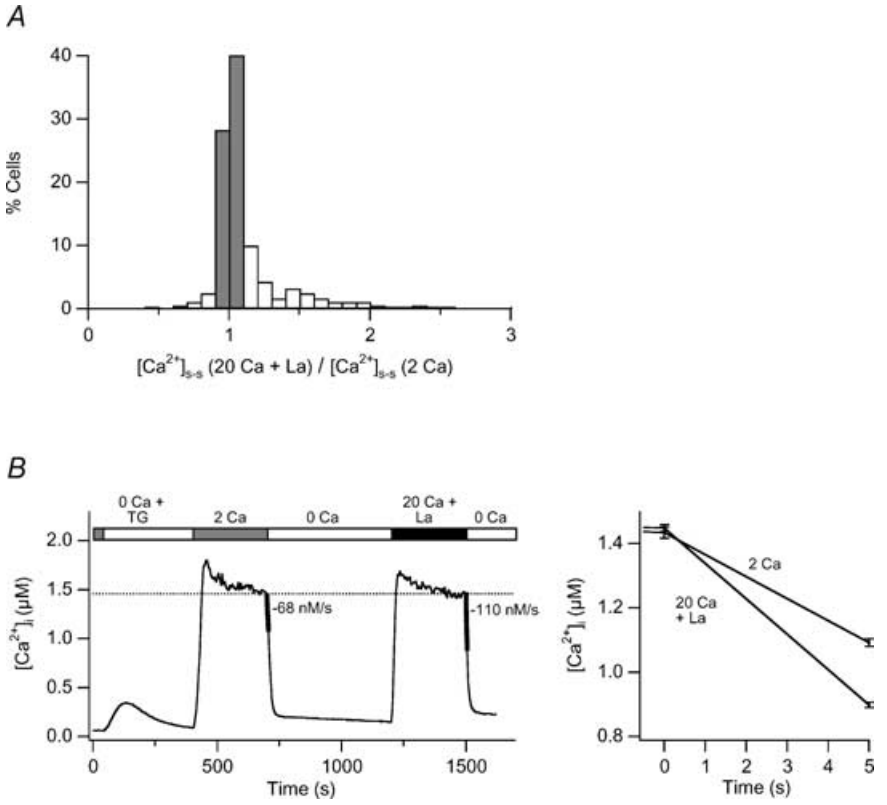

Figure 3. High $[Ca^{2+}]_o$ increases PMCA modulation independently of global $[Ca^{2+}]_i$ in the majority of cells treated with La^{3+} to reduce Ca^{2+} influx
TG-treated cells were exposed to 2 mM $Ca^{2+}{}_o$ or 20 mM $Ca^{2+}{}_o$ + 7 nM La^{3+} as indicated in *B*. *A*, distribution of the plateau $[Ca^{2+}]_i$ levels generated by 20 mM $Ca^{2+}{}_o$ + 7 nM La^{3+} relative to 2 mM $Ca^{2+}{}_o$ in 373 cells. Iso-$[Ca^{2+}]_i$ cells (68% of the population) are indicated by the shaded bars. *B*, average $[Ca^{2+}]_i$ responses from the iso-$[Ca^{2+}]_i$ cells identified in *A*. Ca^{2+} clearance rates measured over a 5 s period are indicated by the thickened lines (left) and are plotted on an expanded scale (right).

activate Ca^{2+}-sensing receptors (CaRs) that can stimulate a variety of intracellular signalling pathways (Brown & MacLeod, 2001), raising the possibility that stimulation of such receptors might contribute to the increased PMCA modulation we observed. Therefore, it is important to test whether increased Ca^{2+} influx through CRAC channels can enhance PMCA modulation at a constant value of $[Ca^{2+}]_o$. To this end, we examined the effects of a low concentration of 2-APB, which is known to enhance CRAC channel activity severalfold, probably by increasing the channel open probability (Prakriya & Lewis, 2001). In this way, 2-APB provides an effective tool to increase Ca^{2+} influx without changing $[Ca^{2+}]_o$.

Acute application of 5 μM 2-APB in 2 mM $Ca^{2+}{}_o$ had similar effects to raising $[Ca^{2+}]_o$ from 2 to 20 mM. On average, PMCA modulation was increased by 1.9-fold with only a modest rise in the steady-state $[Ca^{2+}]_i$ (1.2-fold; Fig. 4*A*). The increased PMCA activity does not appear to reflect a direct effect of 2-APB on the PMCA, for two reasons. First, this low concentration of 2-APB does not alter $[Ca^{2+}]_i$ when applied to resting cells (Prakriya & Lewis, 2001). Second, 2-APB does not affect the time course of Ca^{2+} clearance when added acutely during recovery from a high-$[Ca^{2+}]_i$ plateau (Fig. 4*B*). As in the driving force experiments described above, ~15% of the cells in the population displayed similar steady-state $[Ca^{2+}]_i$ before and after treatment with 2-APB (Fig. 4*C*). 2-APB enhanced modulation in all of these cells, increasing PMCA activity by an average of 1.7-fold (± 0.2, $n = 19$ cells; Fig. 4*D*). The ability of 2-APB to enhance modulation in constant $[Ca^{2+}]_o$ rules out a significant role for CaR in this response and further supports the idea that CRAC channels trigger PMCA modulation through local changes in $[Ca^{2+}]_i$.

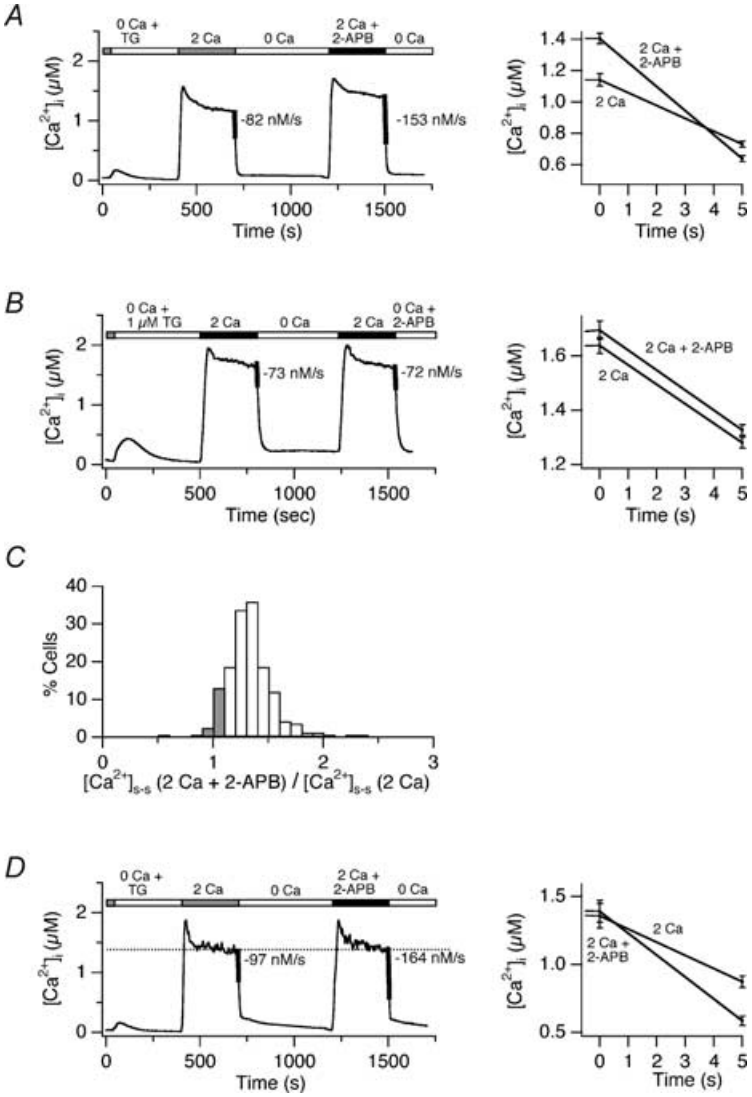

Figure 4. 2-APB enhances PMCA modulation independently of changes in $[Ca^{2+}]_i$ and $[Ca^{2+}]_o$

A, 2-APB increases the rate of Ca^{2+} clearance. Following store depletion with 1 μM TG, cells were exposed to 2 mM $Ca^{2+}{}_o$ for 300 s and following an 8 min recovery period, with 2 mM $Ca^{2+}{}_o$ + 5 μM 2-APB. Slopes during the first 5 s after $Ca^{2+}{}_o$ removal are indicated as thickened lines (left) and on an expanded scale (right). Average response of 112 cells. *B*, 2-APB does not affect pump activity directly. 2-APB (5 μM) was added during the washout of $Ca^{2+}{}_o$. Clearance rates were unaffected, as shown by the equal slopes (thickened lines to the left, expanded scale to the right). *C*, distribution of the plateau $[Ca^{2+}]_i$ levels generated by 2 mM $Ca^{2+}{}_o$ + 2-APB relative to 2 mM $Ca^{2+}{}_o$ alone from the experiment in *A*. Iso-$[Ca^{2+}]_i$ cells are indicated by the shaded bars. *D*, average response of the iso-$[Ca^{2+}]_i$ cells identified in *C* (left). 2-APB enhanced the clearance rate 1.7-fold despite the absence of any change in global $[Ca^{2+}]_i$. An overlay of the first 5 s of Ca^{2+} clearance following applications of 2 mM Ca^{2+} ± 2-APB highlights the different PMCA rates (right).

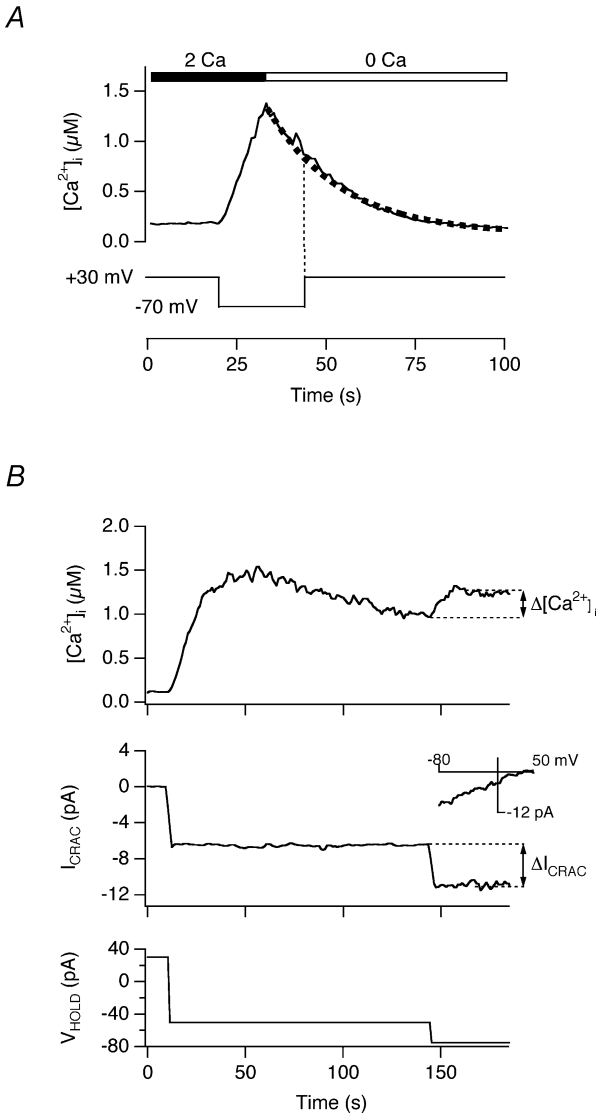

Figure 5. Increasing the electrical driving force for Ca^{2+} enhances PMCA modulation
After establishing the perforated-patch voltage-clamp configuration, single indo-1-loaded cells were treated with 1 μM TG for 10 min to activate CRAC channels at a holding potential of +30 mV to maintain resting $[Ca^{2+}]_i$ levels. Antimycin (2 μM) + oligomycin (2 μM) were present to block mitochondrial Ca^{2+} uptake. *A,* PMCA activity is voltage independent. Hyperpolarization from +30 mV to −70 mV evoked a $[Ca^{2+}]_i$ rise to 1.4 μM in ∼10 s. Subsequent removal of $Ca^{2+}{}_o$ caused $[Ca^{2+}]_i$ to decay back to baseline; the dotted line indicates a single-exponential fit to the recovery phase. Changing the holding potential from −70 to +30 mV did not significantly alter the rate of Ca^{2+} clearance. *B,* hyperpolarization increases PMCA activity with little change in global $[Ca^{2+}]_i$. Hyperpolarization of the holding potential (V_{HOLD}, bottom) evoked an increase in I_{CRAC} (middle, measured at the holding potential) and $[Ca^{2+}]_i$ (top). Leak-subtracted ramp current at −80 to +50 mV (inset) was collected during the period at −50 mV V_{HOLD}. The ramps display the inward rectification and positive reversal potential characteristic of I_{CRAC}. Increasing V_{HOLD} from −50 to −75 mV almost doubled I_{CRAC} with only a slight elevation of $[Ca^{2+}]_i$, implying an increase of PMCA activity.

Hyperpolarization enhances PMCA activity by elevating local $[Ca^{2+}]_i$ near CRAC channels

An effect of local $[Ca^{2+}]_i$ microdomains on PMCA modulation predicts that an increase in Ca^{2+} driving force through membrane hyperpolarization should also enhance modulation independently of changes in $[Ca^{2+}]_o$ and global $[Ca^{2+}]_i$. We tested this prediction in perforated-patch recordings from single TG-treated Jurkat cells loaded with indo-1. To assess whether the membrane potential influences PMCA modulation it is first necessary to verify that it does not directly alter the rate of Ca^{2+} clearance itself; i.e. that PMCA activity is not directly voltage dependent in the absence of Ca^{2+} influx through CRAC channels. In perforated-patch recordings from single TG-treated cells, hyperpolarization from +30 mV to −70 mV caused $[Ca^{2+}]_i$ to rise to levels above 1 μM, and subsequent removal of extracellular Ca^{2+} caused $[Ca^{2+}]_i$ to decay back to baseline with an approximately exponential time course (Fig. 5*A*; similar responses were seen in 4 cells). During the decay, changing the holding potential from −70 to +30 mV did not detectably alter the rate of Ca^{2+} clearance, demonstrating that within this voltage range, and hence at voltages under which our experiments are performed, membrane potential does not directly affect the PMCA flux rate.

We next determined whether increasing the electrical driving force on Ca^{2+} entry enhances PMCA activity independently of changes in $[Ca^{2+}]_i$. As shown in Fig. 5*B*, hyperpolarization of a TG-pretreated cell from +30 mV to a fixed potential of −50 mV evoked a constant increase in I_{CRAC}, identified by its dependence on extracellular Ca^{2+}, inward rectification, low current noise, and reversal potential of > 50 mV (Fig. 5*B*, inset) (Parekh & Penner, 1997; Lewis, 2001). As expected, the ensuing $[Ca^{2+}]_i$ elevation reached a peak and fell to a lower plateau level due to a delayed increase in the rate of Ca^{2+} clearance by the PMCA. Upon reaching the steady-state $[Ca^{2+}]_i$ plateau, the holding potential (V_{HOLD}) was further hyperpolarized to −75 mV, increasing I_{CRAC} from −6.5 pA to −11 pA. Despite the 1.7-fold increase in I_{CRAC}, global $[Ca^{2+}]_i$ increased by only 1.2-fold. Similar behaviour was observed in three cells with varying amplitudes of I_{CRAC} and $[Ca^{2+}]_i$. This behaviour resembles the response shown in Fig. 1*B*, where a comparable increase in Ca^{2+} driving force (via elevation of $[Ca^{2+}]_o$) caused only a small increase in global $[Ca^{2+}]_i$. Thus, to account for the small magnitude of the $[Ca^{2+}]_i$ rise, the hyperpolarization to −75 mV appeared to increase the pump rate by nearly 1.7-fold at a nearly constant global $[Ca^{2+}]_i$. These data further support the

conclusion that the driving force on Ca^{2+}, and hence local $[Ca^{2+}]_i$ gradients, influence PMCA activity.

Discussion

Local $[Ca^{2+}]_i$ microdomains around open CRAC channels contribute to PMCA modulation

The modulation of PMCA activity plays an important role in generating Ca^{2+} dynamics and ensuring long-term stability of Ca^{2+} signals in T cells. In this study, we have shown that increasing the rate of Ca^{2+} influx through CRAC channels can modulate PMCA activity independently of changes in the global average $[Ca^{2+}]_i$. As discussed below, these results argue strongly that local $[Ca^{2+}]$ gradients near CRAC channels contribute to PMCA modulation and that the two proteins are therefore closely coupled on a functional level.

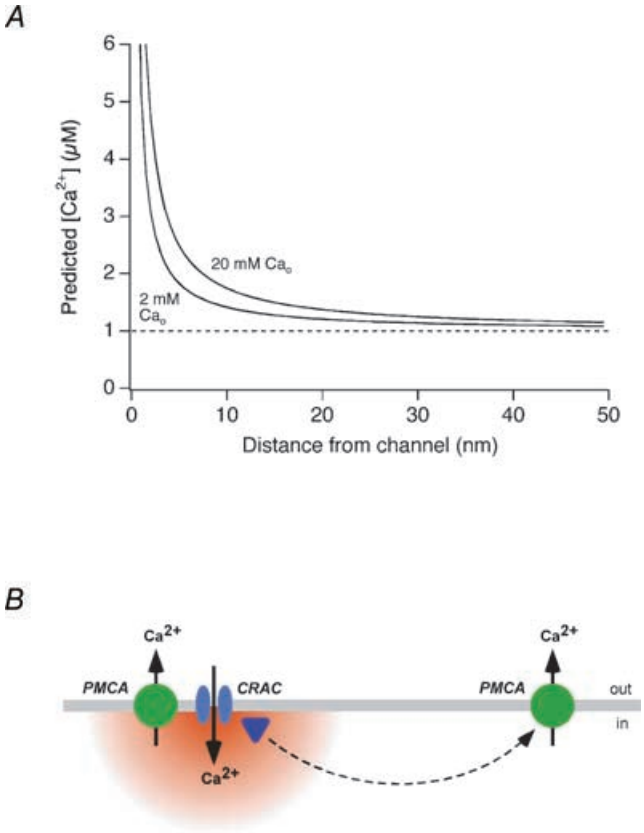

Figure 6. Local $[Ca^{2+}]_i$ gradients near CRAC channels and possible modes of coupling to PMCAs
A, estimate of the $[Ca^{2+}]_i$ gradient in a microdomain around a single CRAC channel using eqn (1) (see text). The 2 mM $Ca^{2+}{}_o$ condition was simulated using a unitary CRAC current of −1.5 fA (Zweifach & Lewis, 1993), and this value was scaled by 1.8 to simulate 20 mM; $Ca^{2+}{}_o$ conditions, based on a K_d for conduction of 2 mM (Premack *et al.* 1994). Global $[Ca^{2+}]_i = 1\ \mu M$; Ca^{2+} diffusion coefficient, $D_{Ca} = 300\ \mu m^2\ s^{-1}$. *B*, possible models for local control of PMCA modulation by Ca^{2+} influx through CRAC channels. Close physical coupling of PMCAs and CRAC channels may expose PMCAs directly to local $[Ca^{2+}]_i$ microdomains which enhance pump modulation. Alternatively, a Ca^{2+} sensor may receive the local Ca^{2+} signal, and via diffusion may modulate PMCAs located at more distant sites.

We considered several alternative explanations for these results other than local control. The increased pump activity during a second application of high $[Ca^{2+}]_o$ is not a consequence of accumulated modulation from the first application, because the order of solution changes did not affect the result, and repeated application of the same $[Ca^{2+}]_o$ did not enhance modulation. The effect is also not due to non-linear intracellular buffering, because the effect occurs in individual cells in which both Ca^{2+} applications evoked the same level of $[Ca^{2+}]_i$. Finally, the effect is not due to activation of CaR by extracellular Ca^{2+}, because it was also elicited by 2-APB and by membrane hyperpolarization, which both increase Ca^{2+} influx in the presence of constant $[Ca^{2+}]_o$. Thus, the simplest explanation consistent with our results is that increased Ca^{2+} influx causes a local increase in $[Ca^{2+}]_i$ that drives the modulation process.

The functional coupling of CRAC channels and PMCAs appears to be a ubiquitous feature of human T cells. When La^{3+} was used to partially block CRAC channels (Fig. 3), increased driving force enhanced modulation in >70% of cells despite a constant level of global $[Ca^{2+}]_i$. It should be noted that this is a lower estimate, because it excludes cells in which global $[Ca^{2+}]_i$ was not identical under conditions of low and high Ca^{2+} driving force. Cells in which high driving force evoked only a slight (20–30%) increase in $[Ca^{2+}]_i$ (Fig. 3*A*) showed a ∼2-fold increase in PMCA activity, suggesting that local coupling operates in these cells as well. In addition, evidence for local coupling was obtained in human T cells from peripheral blood, indicating that the phenomenon is not specific for leukaemic T cells.

Implications of CRAC channel–PMCA coupling for T cell physiology

The close coupling between CRAC channels and PMCAs adds another example to a growing list of cases where store-operated channels interact with their targets through local microdomains. This list includes coupling between store-operated Ca^{2+} channels and adenylate cyclase (Fagan *et al.* 1996, 1998), nitric oxide synthase (Lin *et al.* 2000), volume-regulated anion channels (Lemonnier *et al.* 2002) and mitochondria (Hoth *et al.* 1997). These examples encompass a broad range of physiological end points, but a common consequence of local coupling in each

case is to increase the selectivity of activation of downstream effectors. For example, adenylate cyclase and nitric oxide synthase have been shown to respond selectively to Ca^{2+} flux through store-operated Ca^{2+} channels but not voltage-gated or intracellular Ca^{2+} release channels. Because of the extremely low Ca^{2+} conductance of CRAC channels, local coupling may provide a particularly high degree of specificity in T cells (see below).

The local coupling of CRAC channels and PMCAs also increases the efficiency of modulation, such that the pumps can adjust their rate to changes in Ca^{2+} influx before large changes in global $[Ca^{2+}]_i$ have occurred. In this way, local modulation acts as a governor which limits maximal $[Ca^{2+}]_i$ changes by adjusting the rate of efflux in proportion to the rate of Ca^{2+} influx. An extreme example of this is shown in ~20% of Jurkat cells, in which doubling the Ca^{2+} influx rate fails to change global $[Ca^{2+}]_i$ (Figs 2 and 4). The ability of local modulation to limit rises in $[Ca^{2+}]_i$ also explains the surprising result that low doses of 2-APB cause a robust (3- to 5-fold) increase in I_{CRAC} but only a slight (<10%) increase in global $[Ca^{2+}]_i$ (Prakriya & Lewis, 2001). Thus, local control of modulation provides an extremely effective safety factor to the cell by limiting the maximum steady-state $[Ca^{2+}]_i$ that can result from CRAC channel activation. Further tests of these ideas will require the development of methods for selectively disrupting local communication between pumps and channels without altering global $[Ca^{2+}]_i$.

How does local coupling of CRAC channels and PMCAs arise?

The local functional coupling of CRAC channels and PMCAs could come about in one of two ways. CRAC channels and PMCAs may be close to each other in the plasma membrane, perhaps colocalized through binding to a common scaffold or by association with a common lipid microdomain. Alternatively, local functional coupling might result from a Ca^{2+} sensor localized near the CRAC channel that modulates the PMCAs at a distance, for example by diffusing from the channel to the pump. One possible candidate for such a sensor is calmodulin, which in its Ca^{2+}-bound form can modulate PMCA4b by binding to a C-terminal autoinhibitory domain.

Regardless of which model applies, the spatial extent of $[Ca^{2+}]_i$ gradients near CRAC channels places strict limits on the localization of downstream targets leading to PMCA modulation. A rough estimate of the dimensions of CRAC channel signalling microdomains can be made based on the properties of Ca^{2+} diffusion. Ca^{2+} diffusing freely through a CRAC channel into a cell will create a local steady-state concentration gradient that falls off with distance from the channel:

$$[Ca^{2+}]_i(r) = [Ca^{2+}]_i(\infty) + \frac{i_{CRAC}}{4\pi F D_{Ca} r} \qquad (1)$$

where $[Ca^{2+}]_i(r)$ is the concentration at a distance r from the channel, $[Ca^{2+}]_i(\infty)$ is the global $[Ca^{2+}]_i$, i_{CRAC} is the unitary CRAC channel current, F is Faraday's constant, and D_{Ca} is the Ca^{2+} diffusion coefficient (Neher, 1986). The steady-state condition is appropriate to consider in this case, because at distances of < 20 nm from the channel (see below), steady-state is reached within 200 μs (Neher, 1986), over 10^5 times faster than the modulation process. Figure 6*A* illustrates the predicted profile of $[Ca^{2+}]_i$ within 50 nm of the CRAC channel pore in the presence of 2 and 20 mM $Ca^{2+}{}_o$, assuming a global $[Ca^{2+}]_i$ of 1 μM (the average level in our experiments). This simulation probably underestimates the steepness of the gradient *in vivo*, as it does not include facilitated diffusion afforded by the binding of Ca^{2+} to intracellular buffers. Nevertheless, the simulation illustrates the small dimensions of microdomains likely to exist around CRAC channels due to their extremely low flux rate on the order of 10^4 ions s^{-1} (Zweifach & Lewis, 1993; Prakriya & Lewis, 2002).

The small size of these local $[Ca^{2+}]_i$ gradients implies that PMCAs or the modulation sensor must be intimately associated with CRAC channels in order to sense $[Ca^{2+}]_i$ in microdomains. Because the local $[Ca^{2+}]_i$ contributes significantly to modulation, it must exceed the global $[Ca^{2+}]_i$ of ~1 μM in our experiments. Furthermore, the fact that 20 mM $Ca^{2+}{}_o$ significantly augments modulation over 2 mM $Ca^{2+}{}_o$ in iso-$[Ca^{2+}]_i$ cells implies that the local $[Ca^{2+}]_i$ in 20 mM $Ca^{2+}{}_o$ must also be significantly higher than in 2 mM $Ca^{2+}{}_o$. These criteria appear to be met only at distances of < ~20 nm; uncertainties about the possible cooperativity and absolute Ca^{2+} sensitivity of modulation and the possible clustering of CRAC channels preclude a firm estimate. At these distances, where $[Ca^{2+}]_i$ is in the range of 1–2 μM, only about half of the cell's calmodulin is expected to be fully bound with Ca^{2+} (Persechini & Cronk, 1999), consistent with the ability of increased driving force to augment modulation (e.g. in Figs 2 and 5). A further consequence of Ca^{2+} microdomains is that the degree of local interaction will increase with the driving force on Ca^{2+} (as in Figs 2, 3 and 5) or the open probability of CRAC channels (as in Fig. 4). Under physiological conditions, the open probability of CRAC channels is likely to increase as channels become activated in response to store depletion, and the resulting $[Ca^{2+}]_i$ rise may also enhance the driving force for Ca^{2+}

entry by activating Ca^{2+}-activated K^+ channels and hyperpolarizing the membrane (see Lewis & Cahalan, 1995 for references). In this way the degree of local coupling between pumps and channels may dynamically adjust itself based on the extent of CRAC channel activation.

Local control does not exclude a contribution of global $[Ca^{2+}]_i$ to PMCA modulation in T cells. Because global $[Ca^{2+}]_i$ and the local $[Ca^{2+}]_i$ gradient sum near the channel, even pumps or Ca^{2+} sensors that are linked directly to CRAC channels would be expected to respond to Ca^{2+} from both local and global sources. In addition, a subset of pumps or sensors may be located more distantly and respond primarily to global $[Ca^{2+}]_i$ (Fig. 6*B*). Biochemical approaches will be needed to address this question.

Are PMCAs physically coupled to CRAC channels in T cells?

There is abundant evidence that PMCAs are not localized in a random fashion but rather are targeted to specific locations in cells. In immunohistochemical studies high densities or clusters of PMCAs have been seen in caveolae (Isshiki & Anderson, 1999; Darby *et al.* 2000; Ogi *et al.* 2000), the dendrites, spines and distal soma of cerebellar Purkinje cells (de Talamoni *et al.* 1993; Hillman *et al.* 1996), and hair cell stereocilia (Apicella *et al.* 1997; Yamoah *et al.* 1998). Consistent with these findings, we have also observed punctate staining with the anti-PMCA antibody 5F10 in Jurkat cells (data not shown). In several of these examples, regions of high PMCA density are also rich in Ca^{2+}-permeable channels, suggesting that close physical coupling between the two proteins may serve as a general mechanism for increasing the efficiency of recovery from periods of Ca^{2+} influx.

How could colocalization of pumps and channels arise? If the two proteins are abundant enough, a significant amount of local interaction could result by chance from the random positioning of both proteins in the plasma membrane. Alternatively, local interactions may result from the regulated assembly of multiprotein complexes. While the mechanisms that regulate PMCA organization in the plasma membrane are not known, one intriguing possibility involves scaffolding proteins. PMCA4b is known to interact via a PDZ-binding domain with members of the Dlg subgroup of the membrane-associated guanylate kinase-like (MAGUK) protein family (Kim *et al.* 1998; DeMarco & Strehler, 2001). Dlg proteins are generally thought to mediate the localization and clustering of receptors and to act as a scaffold for the assembly of signalling complexes (Kim *et al.* 1998; DeMarco & Strehler, 2001; Hung & Sheng, 2002). hDlg (SAP97) binds with nanomolar affinity to PMCA4b *in vitro*, and in T cells hDlg has been shown to bind the tyrosine kinase $p56^{lck}$, as well as the voltage-gated K^+ channel Kv1.3 and GAKIN, a novel kinesin-like motor protein (Hanada *et al.* 1997, 2000). Based on these associations and the functional coupling of PMCAs and CRAC channels, it is tempting to speculate that scaffolding proteins like hDlg play a structural role in physically linking PMCA4b with other signalling proteins, perhaps including the CRAC channel, in order to enhance their functional interactions *in vivo*.

References

Almers W & Neher E (1985). The Ca signal from fura-2 loaded mast cells depends strongly on the method of dye-loading. *FEBS Lett* **192**, 13–18.

Apicella S, Chen S, Bing R, Penniston JT, Llinas R & Hillman DE (1997). Plasmalemmal ATPase calcium pump localizes to inner and outer hair bundles. *Neuroscience* **79**, 1145–1151.

Augustine GJ & Neher E (1992). Neuronal Ca^{2+} signalling takes the local route. *Curr Op Neurobiol* **2**, 302–307.

Aussel C, Marhaba R, Pelassy C & Breittmayer JP (1996). Submicromolar La^{3+} concentrations block the calcium release-activated channel, and impair CD69 and CD25 expression in CD3- or thapsigargin-activated Jurkat cells. *Biochem J* **313**, 909–913.

Bakowski D & Parekh AB (2002). Monovalent cation permeability and Ca^{2+} block of the store-operated Ca^{2+} current I_{CRAC} in rat basophilic leukemia cells. *Pflugers Arch* **443**, 892–902.

Bautista DM, Hoth M & Lewis RS (2002). Enhancement of calcium signalling dynamics and stability by delayed modulation of the plasma-membrane calcium-ATPase in human T cells. *J Physiol* **541**, 877–894.

Becherer U, Moser T, Stuhmer W & Oheim M (2003). Calcium regulates exocytosis at the level of single vesicles. *Nat Neurosci* **6**, 846–853.

Bootman MD, Lipp P & Berridge MJ (2001). The organisation and functions of local Ca^{2+} signals. *J Cell Sci* **114**, 2213–2222.

Brown EM & MacLeod RJ (2001). Extracellular calcium sensing and extracellular calcium signaling. *Physiol Rev* **81**, 239–297.

Cannell MB, Cheng H & Lederer WJ (1995). The control of calcium release in heart muscle. *Science* **268**, 1045–1049.

Carafoli E (1991). Calcium pump of the plasma membrane. *Physiol Rev* **71**, 129–153.

Carafoli E (1994). Biogenesis: plasma membrane calcium ATPase: 15 years of work on the purified enzyme. *FASEB J* **8**, 993–1002.

Caride AJ, Elwess NL, Verma AK, Filoteo AG, Enyedi A, Bajzer Z *et al.* (1999). The rate of activation by calmodulin of isoform 4 of the plasma membrane Ca^{2+} pump is slow and is changed by alternative splicing. *J Biol Chem* **274**, 35227–35232.

Caride AJ, Filoteo AG, Penheiter AR, Paszty K, Enyedi A & Penniston JT (2001). Delayed activation of the plasma membrane calcium pump by a sudden increase in Ca^{2+}: fast pumps reside in fast cells. *Cell Calcium* **30**, 49–57.

Darby PJ, Kwan CY & Daniel EE (2000). Caveolae from canine airway smooth muscle contain the necessary components for a role in Ca^{2+} handling. *Am J Physiol Lung Cell Mol Physiol* **279**, L1226–L1235.

Deisseroth K, Bito H & Tsien RW (1996). Signaling from synapse to nucleus: postsynaptic CREB phosphorylation during multiple forms of hippocampal synaptic plasticity. *Neuron* **16**, 89–101.

DeMarco SJ & Strehler EE (2001). Plasma membrane Ca^{2+}-ATPase isoforms 2b and 4b interact promiscuously and selectively with members of the membrane-associated guanylate kinase family of PDZ (PSD95/Dlg/ZO-1) domain-containing proteins. *J Biol Chem* **276**, 21594–21600.

de Talamoni N, Smith CA, Wasserman RH, Beltramino C, Fullmer CS & Penniston JT (1993). Immunocytochemical localization of the plasma membrane calcium pump, calbindin-D28k, and parvalbumin in Purkinje cells of avian and mammalian cerebellum. *Proc Natl Acad Sci U S A* **90**, 11949–11953.

Dolmetsch RE & Lewis RS (1994). Signaling between intracellular Ca^{2+} stores and depletion-activated Ca^{2+} channels generates $[Ca^{2+}]_i$ oscillations in T lymphocytes. *J Gen Physiol* **103**, 365–388.

Dolmetsch RE, Lewis RS, Goodnow CC & Healy JI (1997). Differential activation of transcription factors induced by Ca^{2+} response amplitude and duration. *Nature* **386**, 855–858.

Dolmetsch RE, Pajvani U, Fife K, Spotts JM & Greenberg ME (2001). Signaling to the nucleus by an L-type calcium channel-calmodulin complex through the MAP kinase pathway. *Science* **294**, 333–339.

Dolmetsch RE, Xu K & Lewis RS (1998). Calcium oscillations increase the efficiency and specificity of gene expression. *Nature* **392**, 933–936.

Fagan KA, Mahey R & Cooper DM (1996). Functional co-localization of transfected Ca^{2+}-stimulable adenylyl cyclases with capacitative Ca^{2+} entry sites. *J Biol Chem* **271**, 12438–12444.

Fagan KA, Mons N & Cooper DM (1998). Dependence of the Ca^{2+}-inhibitable adenylyl cyclase of C6-2B glioma cells on capacitative Ca^{2+} entry. *J Biol Chem* **273**, 9297–9305.

Gomez TM, Robles E, Poo M & Spitzer NC (2001). Filopodial calcium transients promote substrate-dependent growth cone turning. *Science* **291**, 1983–1987.

Hanada T, Lin L, Chandy KG, Oh SS & Chishti AH (1997). Human homologue of the *Drosophila* discs large tumor suppressor binds to $p56^{lck}$ tyrosine kinase and Shaker type Kv1.3 potassium channel in T lymphocytes. *J Biol Chem* **272**, 26899–26904.

Hanada T, Lin L, Tibaldi EV, Reinherz EL & Chishti AH (2000). GAKIN, a novel kinesin-like protein associates with the human homologue of the Drosophila discs large tumor suppressor in T lymphocytes. *J Biol Chem* **275**, 28774–28784.

Hillman DE, Chen S, Bing R, Penniston JT & Llinas R (1996). Ultrastructural localization of the plasmalemmal calcium pump in cerebellar neurons. *Neuroscience* **72**, 315–324.

Hoth M, Fanger CM & Lewis RS (1997). Mitochondrial regulation of store-operated calcium signaling in T lymphocytes. *J Cell Biol* **137**, 633–648.

Hung AY & Sheng M (2002). PDZ domains: structural modules for protein complex assembly. *J Biol Chem* **277**, 5699–5702.

Isshiki M & Anderson RG (1999). Calcium signal transduction from caveolae. *Cell Calcium* **26**, 201–208.

Kim E, DeMarco SJ, Marfatia SM, Chishti AH, Sheng M & Strehler EE (1998). Plasma membrane Ca^{2+} ATPase isoform 4b binds to membrane-associated guanylate kinase (MAGUK) proteins via their PDZ (PSD-95/Dlg/ZO-1) domains. *J Biol Chem* **273**, 1591–1595.

Lansman JB, Hess P & Tsien RW (1986). Blockade of current through single calcium channels by Cd^{2+}, Mg^{2+}, and Ca^{2+}. Voltage and concentration dependence of calcium entry into the pore. *J Gen Physiol* **88**, 321–347.

Lemonnier L, Prevarskaya N, Shuba Y, Vanden Abeele F, Nilius B, Mazurier J *et al*. (2002). Ca^{2+} modulation of volume-regulated anion channels: evidence for colocalization with store-operated channels. *FASEB J* **16**, 222–224.

Lewis RS (2001). Calcium signaling mechanisms in T lymphocytes. *Ann Rev Immunol* **19**, 497–521.

Lewis RS & Cahalan MD (1989). Mitogen-induced oscillations of cytosolic Ca^{2+} and transmembrane Ca^{2+} current in human leukemic T cells. *Cell Regul* **1**, 99–112.

Lewis RS & Cahalan MD (1995). Potassium and calcium channels in lymphocytes. *Ann Rev Immunol* **13**, 623–653.

Lin S, Fagan KA, Li KX, Shaul PW, Cooper DM & Rodman DM (2000). Sustained endothelial nitric-oxide synthase activation requires capacitative Ca^{2+} entry. *J Biol Chem* **275**, 17979–17985.

Neher E (1986). Concentration profiles of intracellular calcium in the presence of a diffusible chelator. *Exp Brain Res* **14**, 80–96.

Ogi M, Yokomori H, Inao M, Oda M & Ishii H (2000). Hepatic stellate cells express Ca^{2+} pump-ATPase and Ca^{2+}-Mg^{2+}-ATPase in plasma membrane of caveolae. *J Gastroenterol* **35**, 912–918.

Parekh AB & Penner R (1997). Store depletion and calcium influx. *Physiol Rev* **77**, 901–930.

Persechini A & Cronk B (1999). The relationship between the free concentrations of Ca^{2+} and Ca^{2+}-calmodulin in intact cells. *J Biol Chem* **274**, 6827–6830.

Prakriya M & Lewis RS (2001). Potentiation and inhibition of Ca^{2+} release-activated Ca^{2+} channels by 2-aminoethyldiphenyl borate (2-APB) occurs independently of IP_3 receptors. *J Physiol* **536**, 3–19.

Prakriya M & Lewis RS (2002). Separation and characterization of currents through store-operated CRAC channels and Mg^{2+}-inhibited cation (MIC) channels. *J Gen Physiol* **119**, 487–508.

Prakriya M, Solaro CR & Lingle CJ (1996). $[Ca^{2+}]_i$ elevations detected by BK channels during Ca^{2+} influx and muscarine-mediated release of Ca^{2+} from intracellular stores in rat chromaffin cells. *J Neurosci* **16**, 4344–4359.

Premack BA, McDonald TV & Gardner P (1994). Activation of Ca^{2+} current in Jurkat T cells following the depletion of Ca^{2+} stores by microsomal Ca^{2+}-ATPase inhibitors. *J Immunol* **152**, 5226–5240.

Roberts WM (1993). Spatial calcium buffering in saccular hair cells. *Nature* **363**, 74–76.

Spitzer NC, Lautermilch NJ, Smith RD & Gomez TM (2000). Coding of neuronal differentiation by calcium transients. *Bioessays* **22**, 811–817.

Wang SQ, Song LS, Lakatta EG & Cheng H (2001). Ca^{2+} signalling between single L-type Ca^{2+} channels and ryanodine receptors in heart cells. *Nature* **410**, 592–596.

Yamoah EN, Lumpkin EA, Dumont RA, Smith PJ, Hudspeth AJ & Gillespie PG (1998). Plasma membrane Ca^{2+}-ATPase extrudes Ca^{2+} from hair cell stereocilia. *J Neurosci* **18**, 610–624.

Zweifach A & Lewis RS (1993). Mitogen-regulated Ca^{2+} current of T lymphocytes is activated by depletion of intracellular Ca^{2+} stores. *Proc Natl Acad Sci U S A* **90**, 6295–6299.

Zweifach A & Lewis RS (1995). Slow calcium-dependent inactivation of depletion-activated calcium current. Store-dependent and -independent mechanisms. *J Biol Chem* **270**, 14445–14451.

Acknowledgements

We thank Murali Prakriya, Rick Aldrich, and Ellen Lumpkin for comments on the manuscript, members of the Lewis lab for stimulating discussions, and David Friel for suggestions regarding CaR. This work was supported by NIH grant GM45374 to R.S.L.

Author's present address

D. M. Bautista: Department of Cellular and Molecular Pharmacology, UC San Francisco Mission Bay, San Francisco, CA 94107, USA.